



## Al-Khwarizmi Engineering Journal ISSN (printed): 1818 – 1171, ISSN (online): 2312 – 0789 Vol. 21, No. 4, December, (2025), pp. 13- 31

# Synthesis and Characterization of Flash Graphene for Use in Remediation of Contaminants in Iraqi Groundwater Using Batch Adsorption Techniques

#### Noora Subhi Raheem1\*, and Hayder M Abdul-Hameed2

<sup>1,2</sup> Department of Environmental Engineering, College of Engineering, Baghdad University, Baghdad 10071, Iraq \*Corresponding Author's Email: nawra.sobhi2311@coeng.uobaghdad.edu.iq

(Received 16 January 2025; Revised 31 May 2025; Accepted 3 July 2025; Published 1 December 2025) https://doi.org/10.22153/kej.2025.07.001

#### **Abstract**

This research aims to assess the behavior and effectiveness of flash graphene (FG) in the remediation of pH, EC, total dissolved solids (TDS), cations, and Fe $^{+3}$  from real groundwater (GW) of the wells of the Al-Raeed Research Station, which is used in reclamation and irrigation. enclose that contaminant levels in remediated real GW abide criterion of Iraqis and Food and Agriculture (FAO) standards. Adsorption technology in the batch adsorption mode experiment was achieved by FG, a carbon-based, highly porous structure that has strong adsorption capacity due to its beneficial surface area (71.7 m²/gm). A locally designed and manufactured electroflash reactor was used to synthesize FG by converting activated carbon derived from banana peels. In this process, banana-peel activated carbon (BPAc) was exposed to a mild spark and 8–10 circuit break shocks per reactor run. The FG morphology and functional adsorption groups were characterized via scanning electron microscopy, Fourier transform infrared, and X-ray diffraction tests. The remediation efficiencies in the batch experiments were 69%, 69%, 61%, and 100% for Ca, Mg, TDS, and Fe, respectively, at an optimum FG dosage of 1.5 g, contact time of 4 hours, 150 rpm, and pH of 7. The adsorption capacity, which followed the Freundlich isotherm model, was  $Ca^{+2} = 14.6 \text{ mg/g}$ ,  $Mg^{+2} = 16.4 \text{ mg/g}$ ,  $Fe^{+6} = 0.074 \text{ mg/g}$ , TDS = 7.3 mg/g. Finally, with the synthesized FG used and the parameters (dose, agitation speed, pH, and contact time) adjusted, the batch mode experiments on real GW samples yielded pH, EC, T.D.S.,  $Mg^{+2}$ ,  $Ca^{+2}$ , and  $Fe^{+3}$  values, which satisfied FAO restrictions and Iraqi standards.

Keywords: adsorption; cation; flash graphene; BPAc; groundwater; contaminant; synthesize

#### 1. Introduction

Preserving groundwater (GW) is the aim of many authorities and agencies responsible for water issues to keep GW free of contaminants and to preserve the quality of surface water, and subsequently, ecosystems. Furthermore, the supply of drinkable water in several nations; this GW may also be employed for industry and agriculture [1], in order that the GW supply for irrigation purposes contributes to agricultural output, productivity, and irrigated crop quality [2].

However, rapid technological development, increased pollution, and climate change have

remediation technologies are needed [5].

Physical, chemical, and biological technologies have all been employed to restore GW. Volatilization, ultrafiltration or filtration, incineration, and adsorption are physical methods

resulted in shortage in water resources and marked reduction in water quality [3]. GW resources are considerably vulnerable to anthropogenic pressures.

Direct industrial waste disposal contamination,

landfill leachate, unintentional toxic material spills,

agricultural activities, and overexploitation of aquifers are factors contributing to the depletion of

GW resources. These issues pose a threat to human

health and the environment [4]; thus, investments in

This is an open access article under the CC BY license:



for GW treatment [6]. An efficient technique is adsorption. This technique is known for its straightforward design, high efficiency, and adaptability in terms of use [7]. Adsorption is less costly and can be executed on site, reducing the possibility of contaminants being transported to depollution sites. This process is a good alternative for the recovery of adsorbed minerals from the adsorbent media [8].

Graphene, activated carbon (Ac) (made from various types of agricultural wastes), carbon nanotubes, graphene and its derivatives, flash graphene (FG), and other carbon-based adsorbents have been investigated for GW remediation purposes [9]. Graphene is a carbon-based system comprising a thin two-dimensional substance, one sheet of graphite crystal, and a flexible bond formation. It is composed of three more carbon atoms hybridized with carbon atoms in a honeycomb structure [10].

Two main approaches are used in graphene synthesis: bottom-up and top-down. One technique that is used in the bottom-up approach is the chemical vapor impregnation method [11]. One of the more sophisticated processes is the FG synthesis method, which uses an electric current to flow through the banana peel activated carbon (BPAc) powder. This technique transforms amorphous carbon into graphene by utilizing energy and an electrical discharge [12].

FG structure endows several physical/chemical characteristics, making it useful in adsorption technology to remediate contaminants. Adsorption effectiveness is substantially determined by the surface area, porous structure, oxygen-containing functional and other groups, adsorption circumstances, and adsorbate characteristics, so as an adsorbent FG synthesis and have been extensively studied and effectiveness in aqueous systems, which are manage and identify contaminants more than air and soil pollution remediation [13].

The chemical and physical properties allowed graphene to be used as an adsorbent according to Xu et al. [14]. Sufficiently crystalline or free of imperfections, graphene has a chemically inert surface. Typically, pure graphene's surface engages in physical adsorption ( $\pi$ – $\pi$  interactions) with other molecules. Surface flaws and surface functional groups are typically added to graphene surfaces to increase their reactivity. To adjust the surface and electrical characteristics of graphene, for instance, chemical doping with atoms such as B and N and adding functional groups such as carboxyl, carbonyl, and amine groups, when the number of

layers is odd, a linear band with AB arrangement will appear in few-layer graphene. Intrinsic singlelayer graphene is a zero-gap semiconductor, and its electronic band structure results in electrically conducting and metallic properties. The band structure becomes increasingly complex as the number of layers expands, causing the conduction and valence bands to overlap and many charge carriers to form. FG is used in many sectors, and environmental and health preservation applications. This article discusses the environmental application the remediation of contaminant concentration [11], the insertion of real GW quality parameter values for EC, pH, major cations (K<sup>+</sup>, Na<sup>+</sup>, Mg<sup>+2</sup>, Ca<sup>+2</sup>), major anions (Cl<sup>-1</sup>, SO<sub>4</sub><sup>-2</sup>, NO<sub>3</sub><sup>-1</sup>, HCO<sub>3</sub><sup>-1</sup>), and Fe<sup>+3</sup>, and remediation of (pH, EC, T.D.S., Cations, Fe<sup>+3</sup>) [15].

Wang et al. [16] reported that Cr, Pb, Cd, Cu, and Hg are the most prevalent heavy metals in contaminated water. They also investigated how Cr<sup>+6</sup> was removed from aqueous solution using an indirect reduction mechanism with the help of  $\pi$ electrons on the graphene. Under the conditions of graphene = 1 g/L,  $[Cr^{+6}]$  = 1000  $\mu$ g/L, and pH 7, the graphene showed a quick removal of Cr+6 from the contaminated water with a high removal efficiency and full removal of Cr<sup>+6</sup> within 5 minutes. Graphene generally exhibits a high adsorption capacity on cationic metals and can be used for the adsorption of cationic and anionic metals. High cation values in GW might raise the pH of the soil, causing it to become salty, and the ion exchange events brought on by enriched water, such as the adsorption of Na<sup>+</sup> and the release of Ca<sup>+2</sup> and Mg<sup>+2</sup>, cause soil aggregates to scatter and decrease in permeability. It has a high concentration impact on the physical characteristics of soil (deterioration of soil structure) [17]. High consumption can cause neurological disorders, renal difficulties, and stomach and duodenal ulcers [18]. Excess salt causes plants to wilt because it raises the osmotic pressure of the soil solution [19]. GW salinity is an issue anywhere in the world because it puts human health at risk, reduces agricultural yield and profitability, deteriorates arable land, raises the price of maintaining infrastructure, and alters or destroys ecosystems [20].

Single-step synthesis method of FG, one technique, which is adsorption in batch adsorption mode, developed to improve previous research to remediate the contaminants in real ground water [21]. The green synthesis of graphene sand hybrid (GSH) uses a sustainable carbon source derived from the pyrolysis of low-quality dates, without any negative effects on the environment. This material

is designed to remedy Pb(II)- and TC-contaminated GW, and adsorption technology is adopted to bring the experimental results into practice. The sand was combined with the date juice, heated in an oven at 80 °C until solidified on the sand surfaces, and then placed in furnace and transferred to an N2 carbonized furnace at the rate of 100 ml/min. Heating was progressively conducted to 750 °C for complete graphitization of the date syrup, and the mixture was heated gradually to 10 °C for 0.5 h at a rate of 2.5 °C/min, then to 200 °C at a rate of 3.3 °C/min, and finally to 750 °C at a rate of 9.1 °C/min for 3 h. The resultant carbonaceous and graphenelike substance was termed graphene-sand hybrid (GSH), then the experimental work conducted with the optimal batch conditions for contaminant removal (initial pH, contact time, agitation speed, GSH dosage, and initial concentration) was determined. Different values of pH (TC, pH 2 to 12; Pb[II] pH 2 to 7) and dosages (0.05–1 g/100 ml) were used within a time span of 0-180 min, with different initial concentrations of the contaminants (C<sub>o</sub>, 50–250 mg/l), this research demonstrated that parameters in the batch mode that influenced the removal of Pb(II) and TC by the effective values of these parameters (90 min, 6, 200 rpm, 50 mg/l, and 0.5 and 0.7 g/50 ml/min). The results evidenced by adsorption isotherms (Freundlich and Langmuir models) and kinetic models, that the Langmuir model is seen to fit well and adequately represent the sorption process, and the pseudosecond-order models show a better fit for the experimental data, with a maximum adsorption capacity of 55.4 mg/g and 46.4 mg/g for Pb(II) and TC, respectively The current research, at which the maximum removal

efficiency of Pb(II) (98%) and TC (97%), was noted.

#### 2. Experimental work

#### 2.1. Raw materials

The experiment focused on irrigation and land reclamation using remedied genuine GW. Genuine GW samples were sourced from wells near the Al-Raeed Research Station. Among the many branches of Iraq's Water Resources Ministry is the Al-Raeed Research Station, which focuses on cutting-edge field irrigation research and development. The station, research facility, and reclaimed farmland cover 64 acres at Abu-Ghareeb, which lies 20 km west of Baghdad.

GW from the wells was placed in a sterile 2 l glass container; the water was continuously pumped for 3 h. All initial tests were conducted within 48 h. Once transported to the station laboratory, the samples were stored in a dark, refrigerated container. According to Table 1, samples of GW collected from the Al-Raeed station were first tested for cations, TDS, pH, EC, and Fe levels in the laboratory at the station. The GW composition of other cations, anions, heavy metals is listed in the table.

Standards for irrigation water set by the Food and Agriculture Organization (FAO) and those of the Iraqi river preservation system were then used to compare the outcomes.

The National Center for Water Resources Management conducted a batch adsorption experiment to remediate all laboratory tests (cations, TDS, pH, EC, and Fe) for GW samples treated with FG.

Table 1, Real GW premier values of cations, T.D.S., pH, EC, and Fe from Al-Raeed station

GW samples from AL-Raeed Re	search Station	Iraqi's standards	standards of FAO's limits
contaminant	Contaminant values		
T.D.S. mg/l	5390	2000	2000
Ca mg/l	130	-	-
Mg mg/l	200	-	100
рH	8	6.5-8.4	6.5-8.4
EC Ds/m	3.8	2	3
Fe mg/l	0.618	5	5
Cr mg/l	0.04	0.1	0.1
K mg/l	15.5		2
Na mg/l	1200		920
Cl mg/l	990	350	250
SO4 mg/l	1321	400	200
$NO_3$	10.1	10	10
$HCO_3$	750	-	610
CO <sub>3</sub>	0	-	3

#### 2.2. Materials

The materials used in the batch adsorption mode experiment to remediate real GW samples included acetic acid (CH<sub>3</sub>COOH) of 60.052 gm/mol molecular weight, sodium hydroxide (NaOH) of 39.99 gm/mol molecular weight, and locally collected agricultural waste, i.e., banana peels.

#### 2.3. Equipment

The types of equipment used for preparing the BPAC and the FG in batch adsorption mode are listed in Table 2.

Table 2,
Types of equipment

Types of equipment	•
Name	Company
Electrical balance	Precisa 205°, Switzer Land
pH meter probe	China
Shaker	Julabo Labortechnik GmbH,
	Germany
Furnace	SAFTHERM, China
Electrical reactor	Locally manufactured
Glasswares	China
Conical	China
Pipette	China

### 2.4. Characterization of the adsorbent (flash graphene)

Various techniques were used to characterize FG:

### 2.4.1. Scanning electron microscopy (sem) and energy dispersive x-ray spectroscopy

SEM micrographs show the nanoflowers' morphology, the graphene distribution, and the composite's overall structure, demonstrating the material microstructure and surface morphology [22]. Energy dispersive x-ray spectroscopy is an effective method for determining the chemical structure of graphene and its derived compounds [23].

#### 2.4.2. X-Ray diffraction

The XRD patterns for FG were first investigated to characterize the structural properties (height, diameter, and number of layers) and to characterize the graphene stacking nanostructures, exhibited composites, and crystallographic structure [24].

#### 2.4.3. FT-IR spectroscopy

Graphene stacking nanostructures can be described using this method, which also provides details on their crystallographic structure, stack height, stack diameter, and stack number [25].

#### 2.5. Synthesis of BPAc

Figure 1 shows the banana peels gathered from household garbage. The banana peels were rinsed with distilled water to remove any surface dirt and sun-dried for 3 days [26]. Then, the peels were cut into small pieces that measured 2 × 2 mm.

To transform the banana peels into Ac, they were physically treated through a pyrolysis process (carbonization and activation) for 2 h in a 250 °C furnace. The activation process is normally conducted in the presence of a suitable oxidizing agent, such as steam, for steam carbon dioxide is used, such modification of physical activation technique employing a novel basic media approach to generate Ac with a high surface area and controlled pore structure, then passes N2 gas, nitrogen adsorption is employed to verify the effect of the pore structure on the adsorption properties, the process improve the carbon content, usually up to between 85% and 95% [27].

Physical activation is accomplished by using 1 liter per minute of CO<sub>2</sub> and 1 one liter per minute of N2 for 1 hour for each gas passage, as illustrated in Figure 1. The final amount of Ac obtained from banana peels was 30 g. Figure 2 shows a flowchart representing BPAc synthesis. The BPAc was ground into a powder with a mixer grinder until it reached a particle size of 0.25 mm, as shown in Figure 1. Following cooling to ambient temperature, the carbonized samples underwent rinsing with distilled water, several filtration processes, and subsequent drying in a scorching oven set at 110 °C.



Fig. 1. BPAc synthesized sample of banana peel, dried BP, Ac and crushed Ac

Characteristics of the BP, Ac, and FG testing results are given in Table 3. Data were acquired

from the Ministry of Oil and the Petroleum Development and Research Center's lab.

Table 3, Characteristics of the raw material, local adsorbent, and adsorbent

Properties	Banana peels	Activated carbon	Flash graphene
Surface area, m <sup>2</sup> /g	0.5519	0.5415	71.7
Bulk density gm/cm <sup>3</sup>	0.4905	0.4412	0.4333
Real densities, gm.cm <sup>-3</sup>	1.4442	1.3902	1335

#### 2.6. Synthetization of Adsorbent (FG)

Batch mode adsorption was conducted to remediate cations, TDS, pH, EC, and Fe in GW, with varying premier concentration values. Laboratory analysis confirmed that the real GW premier pollutant concentration complied with Iraqi standards for irrigation use. A valuable agricultural waste product, FG was created from BPAc. Synthesizing the adsorbent for contaminants in GW sample cleanup, FG requires crushing Ac into powder and then using the powdered BPAc to make FG.

#### 2.7. Flash Graphene Synthesization Method

An electrical flash reactor is an equipment that consists of two electrodes of high-voltage electricity connected to a copper wire placed in a Pyrex tube, the BPAc is placed also in the tube surrounding the wire, the electrical reactor is used to produce the FG from crushed BPAc by using the spark of light in the reactor to convert the Ac to graphene [28].

The energy required to convert an amorphous carbon feedstock to 1 g of FG has been previously reported as 7.2-23 kJ, based on the input feedstock type [29], [30].

The electrical flash reactor shown in Figure 2 comprises an electrical source, and the power source is connected to the capacitor cabinet via a circuit breaker CB1. A 220 V AC, 10 circuit breaker is also included with the power supply to provide on/off control; building separate capacitor banks is feasible.

Two copper electrodes attached to flexible output cables are connected to a plumb line; once the designed voltage is achieved across the capacitors, the charge can be released to accomplish the whole closed electrical circle. [31]

CB1 is the power source to charge capacitors and control the spark intensity and for LED luminaires utilized as indicators of instrument charge and status [32]. It provides the system with the voltage required to charge a high-voltage capacitor (460 × 4) via a resistor. The BPAc of the 5 g sample (Figure 3) is placed between two plug electrodes that were further contacted by copper electrodes. An electrical pulse is then discharged through the sample. This pulse causes carbon–carbon bonds to break and rearrange into high-quality graphene [33].

The discharge duration was entered as 2-4 seconds between each spark of light, achieved

manually through breaking the circuit eight to 10 times and blowing on the switch [34].

After the capacitor is charged, CB1 is switched off, leaving the bank charged and prepared for release. Capacitors are stored in a capacitor bank and operated by a solid-state relay.

The capacitor banks are coupled to the kill switch, which is upstream from the sample holder connection. To slow the current and provide more steady electrical control, an inductor is connected in series with the circuit [29]. Figure 4 explains the sample of FG.

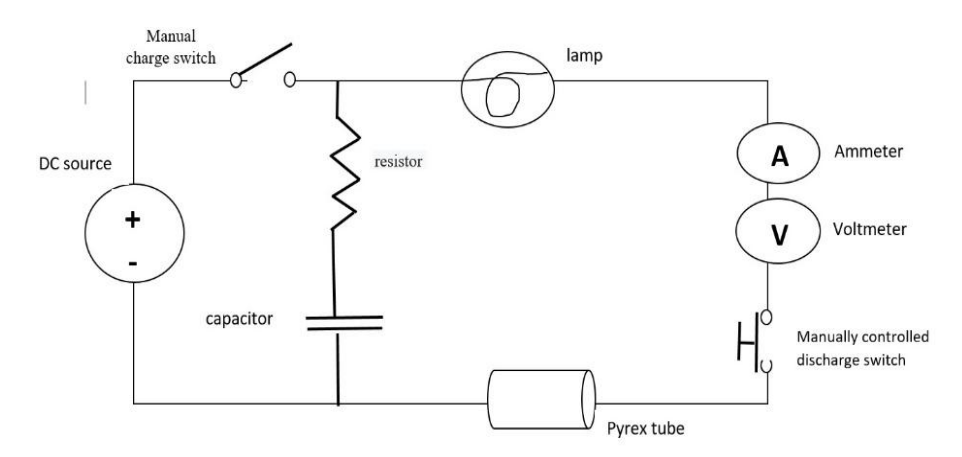


Fig. 2. Electrical flash reactor

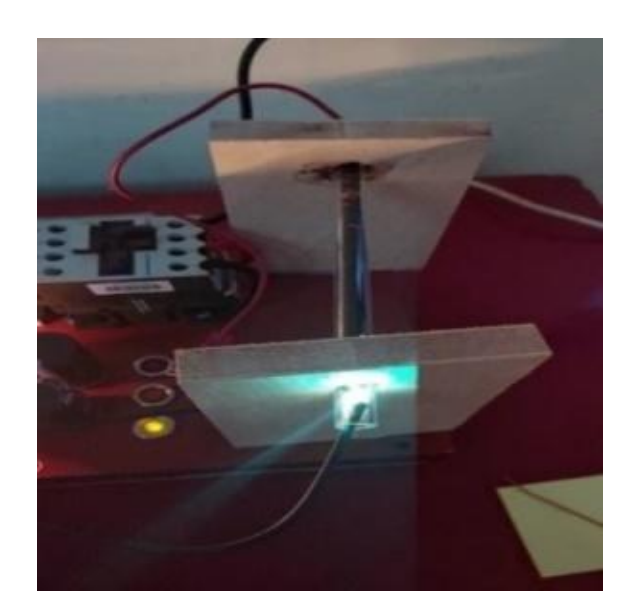


Fig. 3. Synthesized FG Flashlight spark



Fig. 4. Sample of flash graphene.

#### 3. Adsorption experiments

#### 3.1. Batch mode experiment

Analysis of the FG's adsorption capacity was conducted on cations, TDS, pH, EC, and Fe<sup>+3</sup> pollutants in the GW samples to determine the remediation efficacy of this test on real GW.

With one parameter fixed and the others validated, four experiments were performed on the

affected parameters (dosage, pH, time, and rpm), as shown in Table 4. The test operation is applied using the given parameter settings, then the optimal performance is selected. The original GW samples are processed for the lowest contaminant concentration using these operation conditions, which are based on previous scientific research of adsorption studies.

Table 4,

Experiment conditions of adsorption, batch mode

Variables parameters	Values	Constant parameters
Dosage (g)	0.5, 1, 1.5, 2, 2.5, 3	2 h, 200 rpm, pH 7
pН	5, 7, 10	2 h, 1.5 g, 200 rpm
Contact time (h)	1, 2, 3, 4	1.5 g, 200 rpm, pH 7
Agitation speed (rpm)	100, 150, 200, 250	2 h, 1.5 g, pH 7

#### 3.1.1. FG Dose

For each set of adsorption tests, six conical flasks containing 100 ml of GW were filled with varying amounts of FG sorbent. The flasks were then

subjected to contact time, agitation speed, and pH values while being kept at a temperature of 25 °C. For 2 h at 200 rpm, six flasks containing 100 ml of GW sample were mixed with weighted adsorbent of 0.5, 1, 1.5, 2, 2.5, and 3 g, similar to Table 5. Table 6 shows the experiment's remedial outcomes.

Table 5,

FG dosage experiment

Adsorbent	Dosage G	pН	Contact Time H	Agitation speed rpm
	0.5			
	1			200
Elash and bara	1.5	7	2	
Flash graphene	2	/		
	2.5			
	3			

Table 6
Cations, TDS, and Fe+3 conc., pH, and EC values in the dosage experiment results

Dosage of adsorbent (g)	Pollutant Values							
	EC Ds/m	pН	T.D.S. mg/L	Ca <sup>+2</sup> mg/L	$Mg^{+2}$ mg/L	Fe <sup>+3</sup> mg/L		
0.5	4.26	8.65	2726	88	187	0.0766		
1	4.94	8.48	3458	40	170	0.1333		
1.5	3.35	8.52	2144	120	120	0.2085		
2	6.41	8.4	4487	88	187	0.293		
2.5	7	8.43	4900	32	170	0.455		
3	7.8	8.52	5460	32	197	0.5696		

#### 3.1.2. Agitation Speed (rpm)

Batch mode adsorption experiments rely on the agitation speed experiment to find the best speed for remediating the contaminant concentrations and keeping the experiment time to a minimum. Without this experiment, the experiments could take longer.

GW samples with FG dosages of 1.5 gm/100 ml of real GW, pH values of 7 and (2) hours, respectively. At speeds of 100, 150, 200, and 250 rpm, measured the duration that each sample came into touch with the agitation. For a variety of rpm values, Table 7 lists the data of each adsorption experiment.

Table 7, Cations, TDS, pH, EC, and Fe+3 with different agitation speed levels.

(mm)	Pollutant valu	ies				
(rpm)	EC Ds/m	pН	T.D.S. mg/L	Ca <sup>+2</sup> mg/L	Mg <sup>+2</sup> mg/L	Fe <sup>+3</sup> mg/L
100	5.1	8.3	3570	144	43	0.182
150	3.72	7.96	2381	96	62	0.1053
200	3.35	8.52	2144	120	120	0.2085
250	5.72	8.72	4004	355	56	0.3391

#### 3.1.3. Contact Time

Each of the four conical flasks containing 100 ml of GW was filled with 1.5 g of FG as part of the remediation batch mode experiment by adsorption to determine the optimum time to remediate the GW

sample. Afterward, the flasks of 100 ml of real GW were stored in a shaker and vibrated at room temperature with pH = 7 and 150 rpm. Four distinct times (1, 2, 3, and 4 h) were used to prepare the four samples with consistent parameters (rpm, pH, and dose). Each conical flask is shown in Table 8.

Table 8, Cations, TDS, Fe conc., pH, EC values with different periods of contact times

Contact time	Pollutant Va	Pollutant Values							
<b>(h)</b>	EC Ds/m	pН	T.D.S. mg/L	Ca <sup>+2</sup> mg/L	Mg <sup>+2</sup> mg/L	Fe <sup>+3</sup> mg/L			
1	3.66	7.47	2342	144	46	0.123			
2	3.35	7.16	2144	96	62	0.1053			
3	5.51	7.96	3857	216	19	0.1095			
4	3.48	7.29	2227	40	89	0			

#### 3.1.4. Impact of pH of the solution

A 1.5 g sample of FG adsorbent was added to three 100 ml genuine GW samples. The pH values of the samples were confirmed to be 5, 7, and 10, and measurements were made for the solutions'

preparation, contact time (4 h), and rotational speed (150 rpm) for each of the three conical flasks.

Table 9 shows the amounts of sodium hydroxide (NaOH) and acetic acid (CH<sub>3</sub>COOH) that were added to the flasks to maintain the various pH values. The results are also shown in Figures 8 (a–d).

Table 9, EC value, cations, TDS, Fe concentrations for different PH values

pН	pollutant Values				
	EC Ds/m	T.D.S. mg/L	Ca <sup>+2</sup> mg/L	Mg <sup>+2</sup> mg/L	Fe <sup>+3</sup> mg/L
5	5.72	4004	355	56	0
7	3.47	2221	72	120	0
10	3.63	2323	56	106	0.3391

#### 3.2. Adsorption isotherm models

Explains the connection between the concentration of a substance in the equilibrium solution at a constant temperature and the quantity of solute adsorbed [35]

#### 3.2.1. Langmuir isotherm

The adsorptive capacity of different adsorbents is measured and compared using Langmuir adsorption, which was initially developed to characterize solid–solid phase adsorption. The Langmuir isotherm balances the corresponding adsorption and desorption rates [36].

The linear form of the Langmuir equation is

$$Ce/qe=(1/(qm\times KL))+(Ce/qm), \qquad ...(1)$$

where Ce is the adsorbate's concentration at equilibrium (mg/l), qmax is the quantity of molecules adsorbed on the adsorbent's surface at any time, and maximum adsorption capacity (mg/g) and KL Langmuir constant (l/mg).

#### 3.2.2. Freundlich isotherm

Hardly a large variety of adsorption values may be used with this adsorption isotherm model. Plotting log qe versus log Ce yields a straight line with 1/n as the slope and log (KF) as an intercept, indicating the variables of this isotherm model [37].

The nonlinearized form is

$$qe = KF Ce \times 1/n. \qquad ... (2)$$

The linearized form is

$$\log qe = \log KF + (1/n \times \log Ce). \qquad ... (3)$$

### 4. Results and Discussion 4.1. Adsorption

FG has the potential to be a valuable tool in batch adsorption techniques for decreasing real GW pollutants due to its exceptional features, including its light weight, high flexibility, chemical stability, huge specific area, and robust tensile strength. The vast majority of these composites' possible applications are in electrical or catalytic reactions, as mentioned in [9]. Environmental remediation is a frequently used and important application of bulk carbon [38]. The capacity of a solute to adsorb onto an adsorbent is heavily dependent on two primary parameters: surface chemistry and pore density. Ion exchange, hydrogen bonds, electrostatic bonds, van

der Waals forces, and countless other types of bonds can be formed when particles with opposite charges engage with one another [39]. The  $\pi$  electrons of the carbocyclic six-membered ring were found to aid in the indirect reduction process of iron from an aqueous solution. GW also includes trace amounts of inorganic cations such as magnesium and calcium. Given the high amounts of these cations in the original GW, any contamination must be removed. Cations were adsorbed onto graphene due to their positive charge [40].

According to the test results, cations (Ca+2, Mg+2), TDS, pH, EC, and iron (Fe+3) were all revived in the GW samples. Using a 1.5 gm/100 ml GW sample of FG for 4 h, adsorption batch mode tests were performed to investigate the critical parameters for pollutant adsorption onto the adsorbent. FG was made from BPAc. According to Table 8, the solution has a pH of 7 when spun at 150 rpm.

### 4.2. Flash graphene characterization 4.2.1. SEM and EDX

The adsorbents' defined, rough, and exceedingly porous surface morphologies are demonstrated in Figure 9, indicating their suitability for adsorption [41]. It demonstrates that graphitic nanoparticles can initiate the nucleation and growth of graphitic crystals by creating a bed for them. When the SEM pictures of FG in (a) and (b) are combined, a continuous graphitic shell is eventually produced [42]. For this study, when analyzed FG using SEM. Its structure is rife with creases and flaws, and its outer layer is noticeably thicker than the rest.

In Figure 6, FG sheets represent representative shots of SEM; between hundreds of nanometers to many microns, the sheet size varies considerably. When exfoliated to single-atom thicknesses using a detergent, these vast sheets may produce an enormous aspect ratio, which has a considerable effect on the characteristics of the resultant nanocomposite to enhance the adsorption capacity of FG [34].

The EDX spectra were collected from the lateral size ( $\sim 1000~\mu m^2$ ) area of FG on the substrate, taken with the electron beam energy of 20 KeV. The synthesis stage of FG produces a large external surface with sufficient pores [43]. Results of the EDX spectrum show the presence of elemental contents of C, O, Si, P, K, Cl, Ca, N (wt.%), respectively for FG samples of 45.68%, 35.93%, 1.32%, 1.07%, 10.6%, 5.4%, 11.89%, 7.2%, as shown in Figure 5.

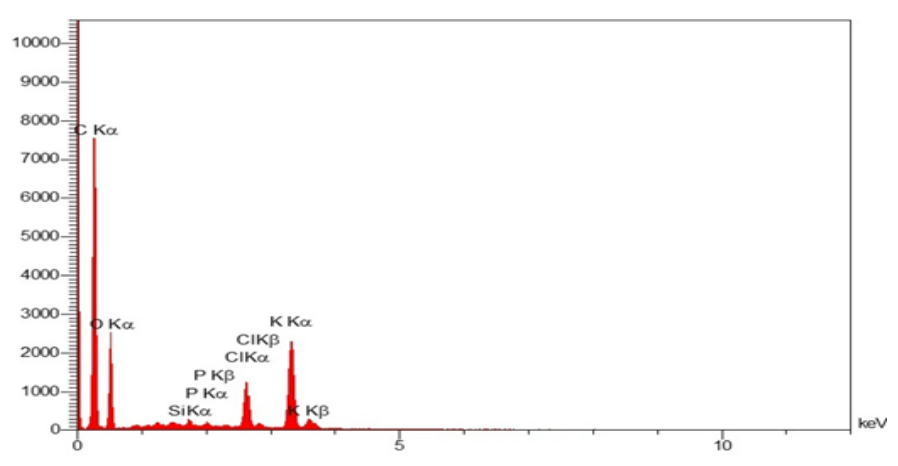


Fig. 5. EDX spectrum analysis of FG

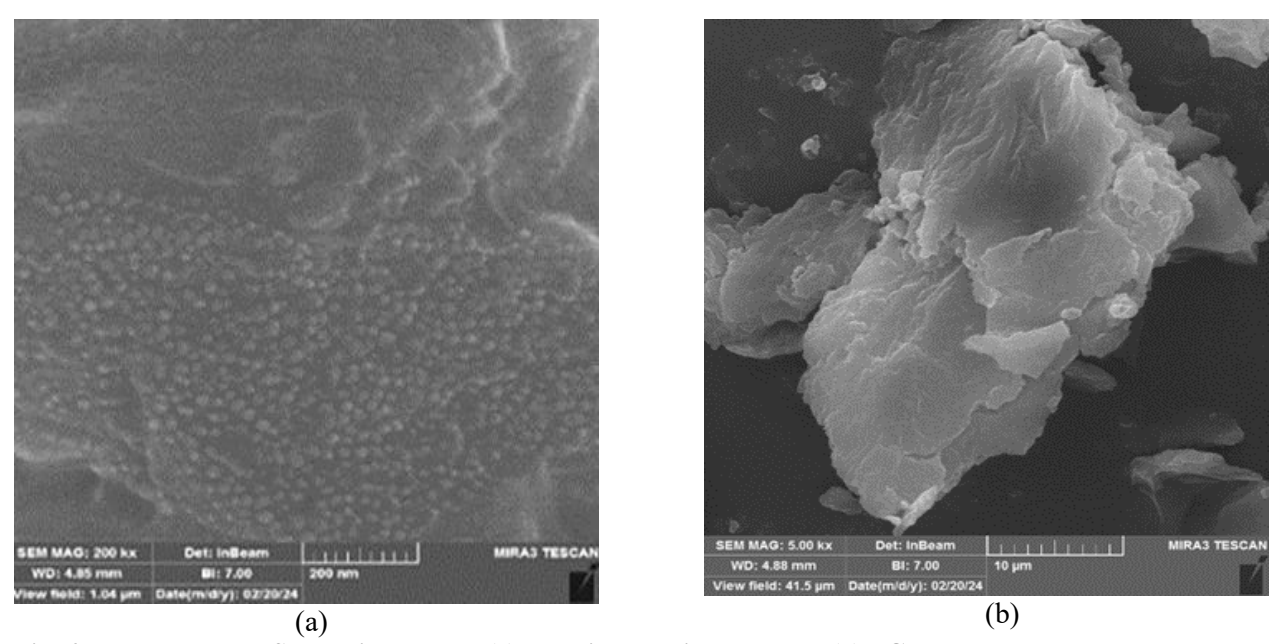


Fig. 6. Flash graphene SEM micrographs (a) spherical particulate seeds (b) FG layers shells developed upon seeds

#### 4.2.2. XRD

The commercial (raw) graphite's XRD spectra, which showed an average particle size (d50) of 111 mm. With a d-spacing (interlayer spacing) of 3.36 Å in, the distinct characteristic sharp peak for graphite appears at  $2q\sim26^{\circ}$ . The intense XRD peaks show that the material is extremely crystalline and that the size reduction is unaffected by the crystalline structure of graphite. Graphite's crystal size, as determined by the Scherrer equation with the (002) plane in mind, is 37.5 nm [44].

Figure 6 displays the synthesized graphene's XRD. FG is between the crystalline and amorphous

forms of structure, which increases the adsorption capacity. This increase is demonstrated by the appearance of the diffraction line with the high peak at  $2\theta$  and the weak (001) peak at  $28.5^{\circ}$  and  $40.7^{\circ}$  in the  $2\theta$  values [45], which suggest statically supported graphene. which shows the separation between graphene layers and implies statically stabilized graphene. A two-dimensional structure incompatible with layers by translation or rotation, and with the interlayer spacing, which defines statically supported graphite. That of crystalline graphene (0.335 nm) is comparable. Figure 7 shows a large peak at a  $2\theta = 13^{\circ}$  [24].

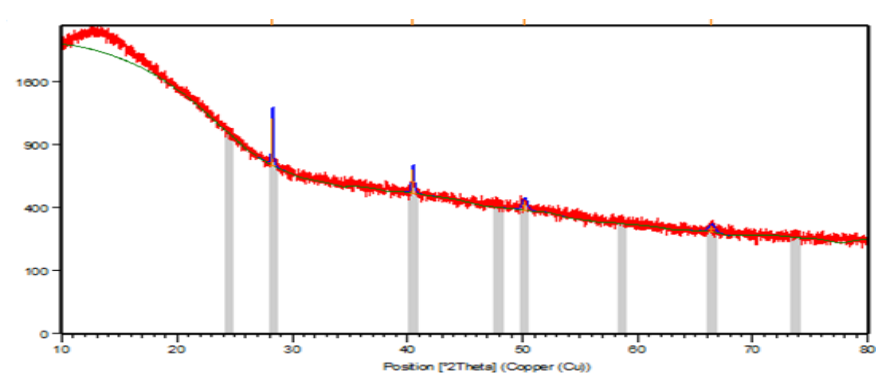


Fig. 7. X-ray diffraction (XRD)

#### 4.2.3. FTIR

Figure 8 shows the graphene FTIR spectra. The reflectance mode was used to capture the FTIR spectra inside the 4500–600 cm<sup>-1</sup> spectral region at a resolution of 4 cm<sup>-1</sup>. The chemical functionalities that caused the adsorption were located in the 1600–1400 cm<sup>-1</sup> range. Carbonyl (C=O), the polyacrylamide molecule (C-H) at 891 cm<sup>-1</sup>, and the hydroxyl group at 3000 cm<sup>-1</sup> are all potential contributors to the 2300 cm<sup>-1</sup> peak. The vibrations of the FG structure are amplified by these clusters.

A broad band in the stretching vibrations of the hydroxyl group, which can be OH from carboxylic groups, correspond to the hydrogen-bonded OH groups of dimeric COOH groups and intramolecular bound O-H stretching. These –OH and –COOH group on the surface make graphene become negatively charged when they are dispersed in water, allowing them to form electrostatic bonds with poly cations [46]. It occurs between about 3800 and 3200 cm<sup>-1</sup>, which is an example of functional groups displayed in the structure. The FG FTIR spectra reveal the presence of several chemicals that are produced from oxygen. Adsorption can only take place when these functional groups coordinate their efforts [47].

Simple alkyl-substituted anhydrides (-COOR) and stretching in carboxylic acids (-COOH) generally give bands near 1970 and 1788 cm<sup>-1</sup>, denoted to carbonyl groups (C=O). Vibrations of three bands can be identified at 1630 cm<sup>-1</sup>, unconjugated carbonyl (C=O), and 1593 cm<sup>-1</sup> imine (C=C). The symmetric stretching of the C-O bonds in COO- seems to be responsible for the peak at 1386.92 cm<sup>-1</sup>. One can see a broad band at 1055.97 cm-1. Possible causes include of C-O bonds. Not only are these little peaks unique to cellulose, but so is the peak (648.34–580.93) cm<sup>-1</sup>, which could be caused by out-of-phase ring stretching [48].

Following the incubation of cations, the FG FTIR spectra essentially retain the same throughout

the process. The primary reason for the difference spectrum's negative band around 1600 cm<sup>-1</sup> is a reduction in the level of trapped water. Some C–O functional groups may be in charge of the cations' adsorption of FG at low pH, as evidenced by a minor increase in intensity of the band centered at 1055 cm<sup>-1</sup>, which corresponds to the cations+ associated C–O stretching. Such stretching mode of tertiary or aromatic alcohols, such as phenol, may begin to deprotonate and participate in the adsorption of cations because FG is known to have a substantial number of phenol and hydroxyl groups attached to the basal plane [49].

Possibly, the 1-methyl-2-pyrrolidinone treatment added CH2 and C-N groups to the graphene surface, causing the bands at 1410 and 1102 cm<sup>-1</sup>. Hydrogen peroxide and sulfuric acid, an oxidation reagent, promote the stretching of amidetype C-O bond, which causes the band at 1631 cm<sup>-1</sup>. Attached to the band at 2925 cm<sup>-1</sup> is CH3 stretching groups from the organic solvent of 1-methyl-2pyrrolidinone. C-H bending is reflected by the 795 cm<sup>-1</sup> band and the N-H bending by the 643 cm<sup>-1</sup> band.[38]. A structural change is induced by the matching functional groups as the peak displacement decreases. The GW pollutants, including cations, TDS, pH, EC, and Fe<sup>+3</sup>, have been adsorbed, as indicated by this change.

Thus, the hydroxyl and carbonyl groups are crucial for the adsorption of the ions because their loading bands shifted to lower displacement. Cations may move through the FG and engage with the negatively charged carboxyl and hydroxyl groups on the surface of the nanosheets. The zeta potential of FG is normally 30 mV in bulk water at neutral pH. Given their more considerable contact with FG surface groups, divalent ions are also good cross-linkers across arranged sheets. demonstrated by the formation constant (stability constant) for cations+ complexes with ligands that include carboxylic moieties [50].

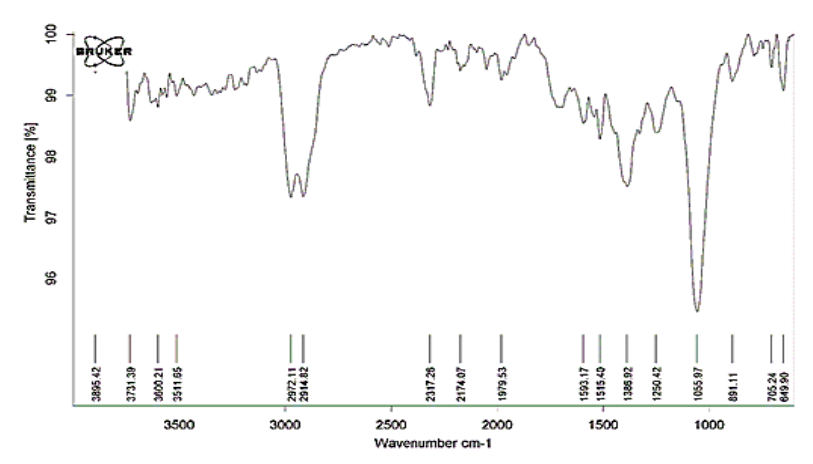


Fig. 8. FTIR of flash graphene

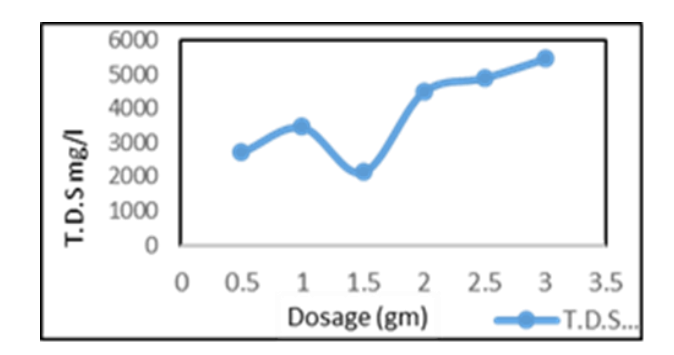
### 4.3. Remediation of Real GW for irrigation and reclamation purposes

When compared to Iraqi and FAO standards, the actual site wells' GW that were first evaluated fell into the categories of moderate and inappropriate levels for GW (cations and Fe) and inappropriate levels for GW (TDS) for irrigation and reclamation purposes. As a result, using untreated GW for irrigation harms crops and lowers output.

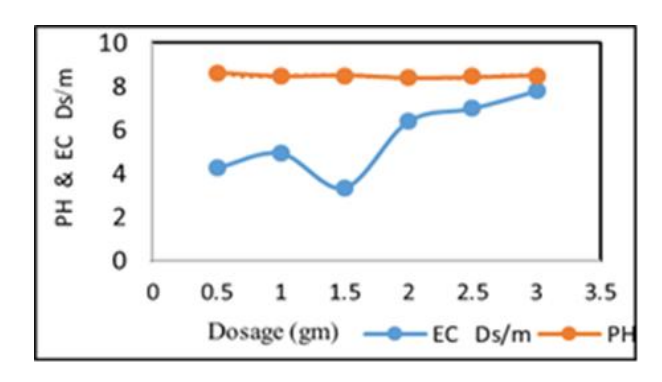
The results of adsorption batch mode experiments at optimum parameters measured and based on the lowest concentrations of the contaminant (cations, TDS, pH, EC, and Fe) that are reached to 0 mg/L of Fe which demonstrate that at high level for any other case of contamination with FE could be remediate to match standards, when compared to Iraqi and FAO's limitations, illustrate that the benefits of employing FG as an adequate adsorbent in one of the GW remediation techniques to reduce crop and production damage can be validated using the GW that was remediated by this lab experiment.

### 4.4. Impact of batch experiment parameters 4.4.1. Impact of FG Dosage

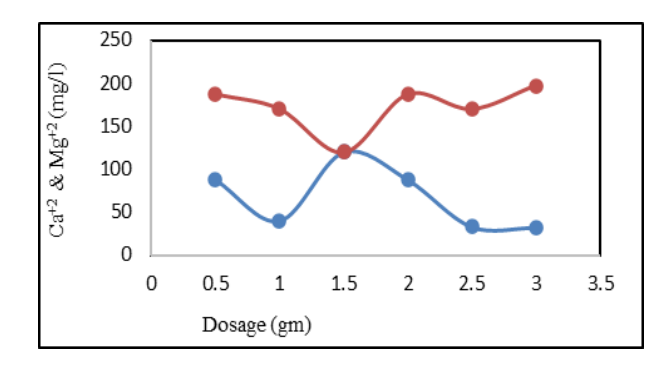
An increase in the adsorbent dosage increases the quantity of cations, Fe<sup>+3</sup>, TDS eliminated. This spike can be connected to the increasing quantity of active sites for FG that are accessible when the dose is raised. The FG dose value of 1.5 g/100L of real GW produced the best removal value. Additional dosage did not lead to improvement, which can be explained to the overlaying of particles. Figures 9 (a–d) provide a graphic representation of the experimental results [47].



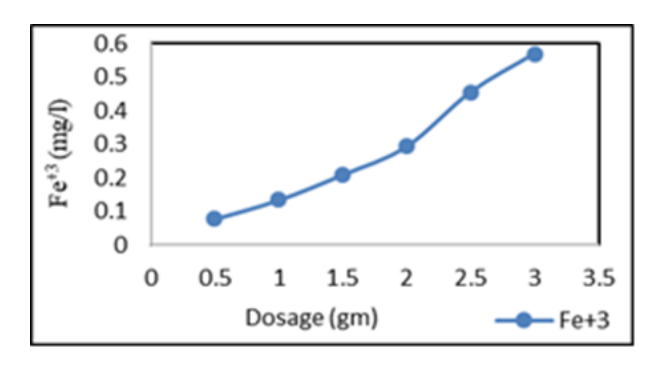
(a) TDS mg/l conc. and dosages (gm)



(b) pH & EC Ds/m values and dosages (gm)



(c) Ca<sup>+2</sup> and Mg<sup>+2</sup> mg/l conc. and dosages (gm)

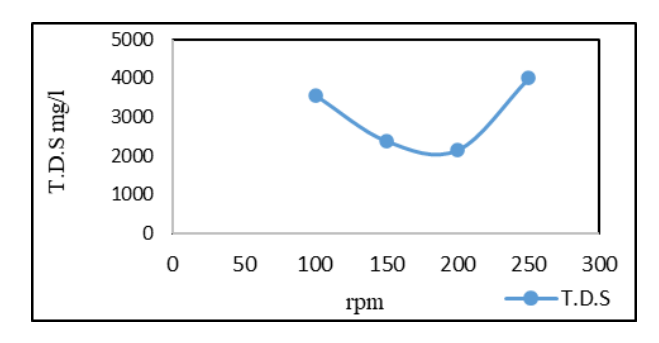


(d) Fe<sup>+3</sup> mg/l conc. and dosages (gm)

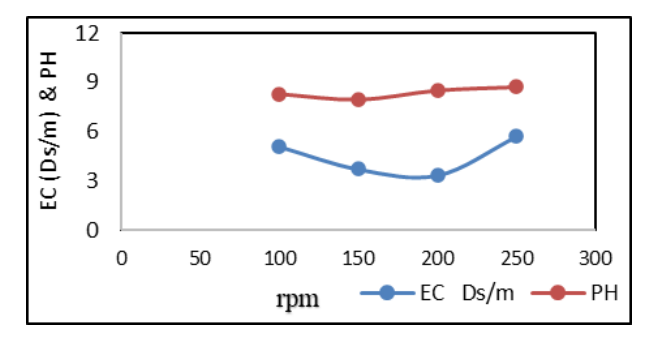
Fig. 9. Impact of different dosages of FG used

#### 4.4.2. Impact of agitation speed

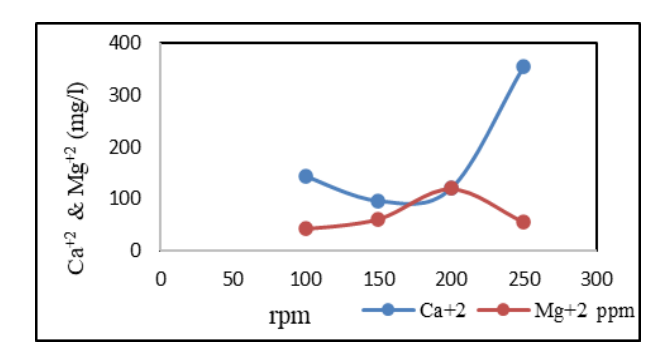
An agitation speed of 100, 150, 200, and 250 rpm affects FG's adsorption of cations, Fe<sup>+3</sup>, and TDS. The plot indicates that an increased agitation speed resulted in an increased adsorption by FG and the optimum contaminants at 150 rpm. The cause was that when the Ca<sup>+2</sup>, Fe<sup>+3</sup>, and TDS ions navigate the boundary layer and approach the solid phase, they come against resistance at the liquid phase. However, for Ca<sup>+2</sup> ions, optimum agitation speed at 200 rpm, where at the boundary layer dropped as a result of the mixture's increased agitation, which reduced resistance in the liquid phase and the adsorbent's capacity to absorb impurities [51]. Figures 10 (a, b, c, and d) depict the experiment's results.



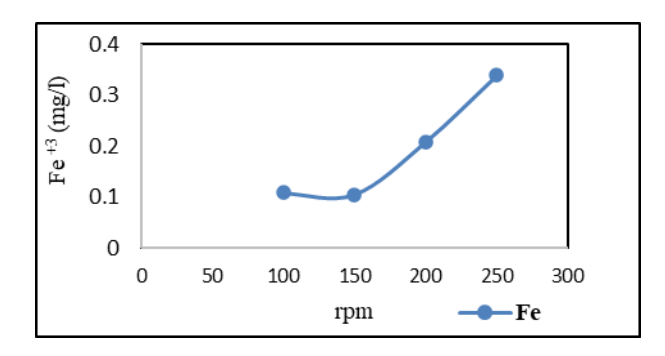
(a) TDS (mg/l) values and agitation speed (rpm)



(b) EC Ds/m and pH values and agitation speed (rpm)



(c) Ca<sup>+2</sup> & Mg<sup>+2</sup> (mg/l) conc. and agitation speed (rpm)

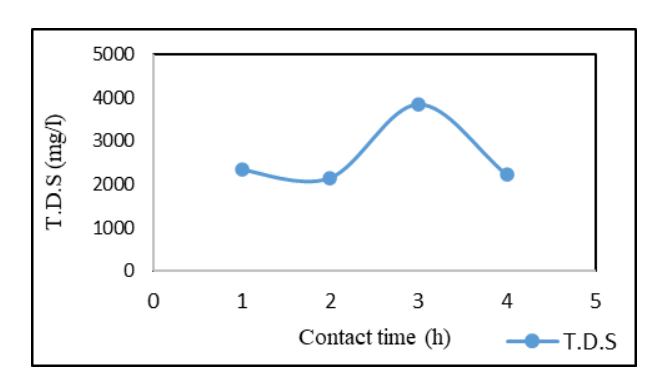


(d) Fe<sup>+3</sup> (mg/l) conc. and agitation speed (rpm)

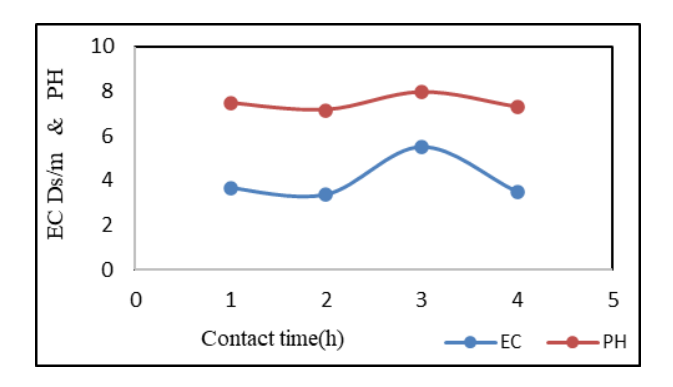
Fig. 10. Impact of different rpm levels

#### 4.4.3. Impact of contact time

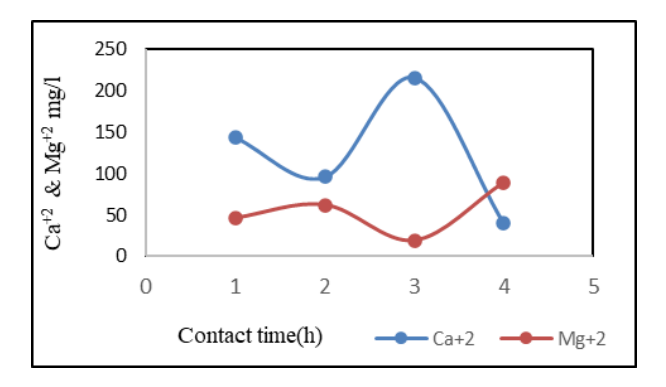
The adsorption of Ca<sup>+2</sup>, Fe<sup>+3</sup>, and TDS, which is the ideal adsorption time at 3 hours, decreases as a result of the decrease in adsorption sites and concentration gradient. The increase in the pace of adsorption after 3 h may be attributed to the fact that initially, all adsorbent FG sites are empty and the concentration gradient is high. Then, it became at maximum uptake on the FG surface [52]. These fundamentals represented in Figure 11. (a, b, c, and d)



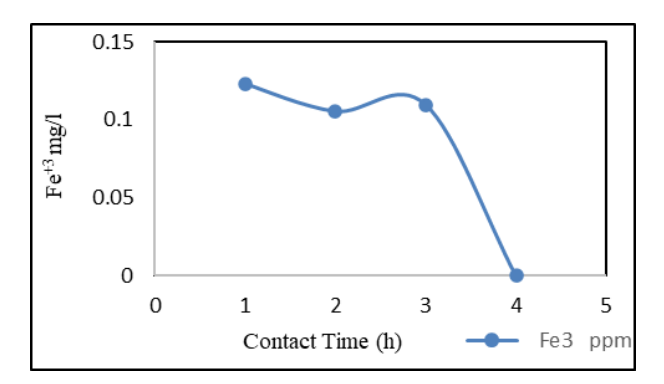
(a) TDS mg/l conc. and contact time (h)



(b) EC Ds/m and pH values and contact time (h)



(c) Ca<sup>+2</sup> & Mg<sup>+2</sup> mg/l conc. and contact time(h)

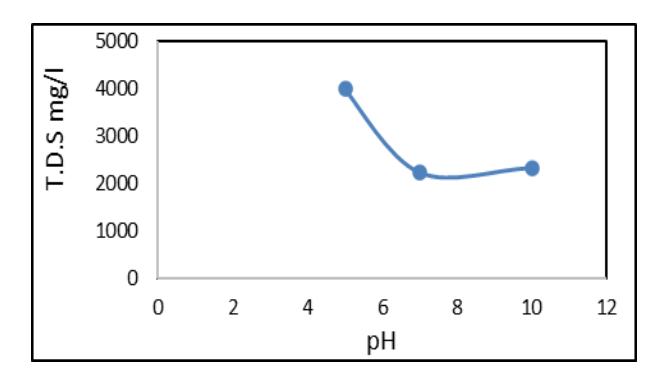


(d) Fe+3 mg/l conc. and contact time (h)

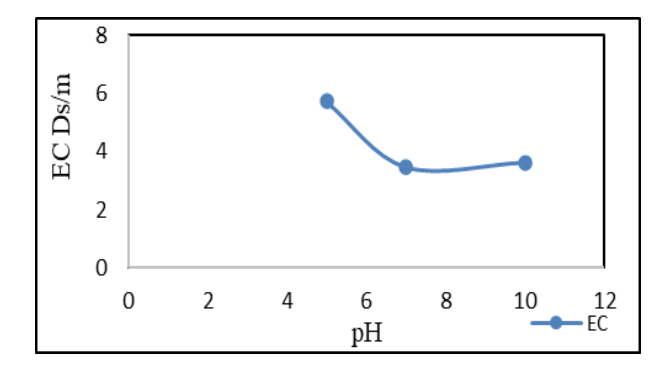
Fig. 11. Impact of variable periods of contact time.

#### 4.4.4. Impact of pH levels

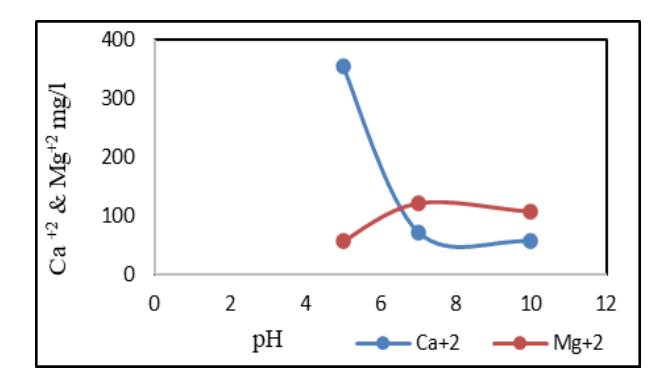
Due to the high concentration of H+ ions at low and modirate pH levels, which neutralize the negatively charged hydroxyl group (OH-) on the adsorbed surface and reduce the resistance to the diffusion of ions, a higher adsorption capacity occurred at lower pH levels, with an optimal range of pH = 5 and pH=7 for Mg<sup>+2</sup> ion. The concentration of OH ions at higher pH levels at pH=10 may make it feasible for adsorption to decrease because they raise the resistance ion transport [53]. As it represented in Figure 12.



(a) T.D.S. mg/l conc. and pH levels



(b) EC Ds/m value and pH levels



(c) Ca<sup>+2</sup> & Mg<sup>+2</sup> mg/l conc. and pH levels

Fig. 12. Impact of variable pH levels

### 4.5. Langmuir and freundlich isotherms 4.5.1. Langmuir adsorption

It includes four preconceptions.

- (1) The surface of the adsorbent is homogenous, and practically every binding site is identical to one another.
- (2) The molecules that are adsorbed do not come into contact with one another.
- (3) The adsorption process is equivalent.
- (4) maximum monolayer adsorption [36].

#### 4.5.2. Freundlich adsorption

It applies to heterogeneous and multilayer molecule adsorption and explains the surface's

heterogeneity and the active site's exponential distribution and energy [54]. Parameters of both adsorption models (Langmuir & Freundlich) fitting the data of adsorption equilibrium listed in Table 9.

Table 9, Langmuir, Freundlich model parameters of adsorption capacity for cations and TDS.

Adsorption isotherm	Parameter	Ca <sup>+2</sup>	Mg <sup>+2</sup>	Fe <sup>+3</sup>	TDS	
Langumir model	$q_{max}$	14.6	16.4	0.0074	7.6	
	$K_L$	0.054	0.0089	12.6	0.004	
	$\mathbb{R}^2$	0.82	0.22	0.33	0.56	
Frendeulich model	1/n	0.86	0.205	0.883	0.312	
	$K_{\mathrm{f}}$	0.16	0.0089	0.132	0.001	
	$\mathbb{R}^2$	0.95	0.72	0.63	0.88	

The Freundlich isotherm in the experimental data exposes fitting better than Langmuir, as the value of  $R^2$ , Freundlich >  $R^2$  Langmuir, indicating that adsorption of cations, TDS, and  $Fe^{+3}$  is chemisorption with multilayer sorbents at a heterogeneous surface of FG.

#### 4.6. Environmental impact

This process creates FG from various carbonaceous solid wastes. Approximately 2 billion tons/year of municipal solid waste is produced worldwide, which is increasingly out of control. Recycling, composting, anaerobic digestion, incineration, gasification, pyrolysis, and landfill disposal are some of the waste management techniques. However, landfills or open dumps end up receiving around 70% of the world's trash. Therefore, a technology that can reduce the amount of garbage or turn waste into useful substance is needed. Waste volume is reduced, and FG is produced as a result of the electroflash reactor's thermal treatment process [55].

The detrimental effect of biomass-based FG synthesis technologies on climate change ranges from 2.73 g to 11.5 g CO<sub>2</sub>e per g of FG generated. These calculations consider the fossil fuel offset from the usage of biogas obtained from the electroflash reactor operations and the carbon captured in the FG. The impact of graphene generated by conventional methods on climate change is far greater than these (149–407 g CO<sub>2</sub>e at the lab scale and 28–407 g CO<sub>2</sub>e at the commercial scale, respectively). This result is mostly due to the fact that electroflash reactor methods utilize considerably less power and chemicals [56] [4].

#### 5. Conclusion

The electroflash reactor method for producing FG can be used to transform waste into high-quality turbostratic graphene. This method's compatibility with various carbon precursors eliminates the need for chemical pretreating, buffer gases, substrates, or graphene washing, demonstrating its enormous potential as a scalable and economically viable synthesis method. One way to improve the environmental benefits of employing agricultural waste is to scale up the process of making flash FG from various carbonaceous sources and to focus on refining the process parameters.

The FG adsorption batch experiment aimed to determine if graphene could remove anions, cations, and heavy metals and to remediate pH, TDS, and EC for GW's agricultural and reclamation applications. The optimum conditions in batch adsorption experiments to remediate real GW are as follows: dosage of  $FG = 1.5 \, g$ , contact time = 4 h, agitation speed = 150 rpm, and pH = 7. These conditions result in a remediation efficiency of 69%, 69%, 61%, 100% for Ca, Mg, TDS, and Fe, respectively.

The adsorption capacities of FG (maximum capacity) at batch adsorption mode experiments, which followed the Freundlich isotherm model, are  $Ca^{+2} = 14.6 \text{ mg/g}$ ,  $Mg^{+2} = 16.4 \text{ mg/g}$ ,  $Fe^{+6} = 0.074 \text{ mg/g}$ , TDS = 7.3 mg/g),

Graphene is a multipurpose material with many potential uses. In the future, researchers may investigate its potential as a water filter for purposes other than drinking and industrial processes.

Future research might incorporate more variables that improve GW and wastewater remediation processes, such as irrigation-related parameters (e.g., temperature and new pH level values), and other pollutants.

More extensive consideration of the ecological effects of graphene synthesis is required. Graphene, a crystalline aggregation of graphite that occurs naturally, is abundant in coal. Researchers in academia and industry should focus more on investigating the retention and degradation of graphene manufacturing on a bigger scale as its use grows.

#### **Greek Letters**

μm Micrometer

 $\pi$  P

#### **Subscripts**

Ac Activated carbon AC Alternating current

PBAc Banana peel activated carbon

CB1 Circuit break 1

FAO Food and Agriculture Organization

FG Flash graphene

FTIR Fourier transform infrared spectroscopy

GW Groundwater

LED Light-emitting diode ppm Parts per million RPM Revolution per minute

SEM Scanner Electron Microscopy

T.D.S. Total dissolved solids

V Volte

XRD X-ray diffraction

Nm Nanometer

#### Acknowledgements

The National Centre for Water Resources Management, an agency of the Iraqi Water Resources Ministry, and the AL-Raeed research stations are providing support for this effort. University of Baghdad's College of Engineering's Environmental Engineering Departments are funding this project.

#### References

[1] W. Hassan, et al., "New composite sorbent for removal of sulfate ions from simulated and real

- groundwater in the batch and continuous tests," Molecules, vol. 26, no. 14, p. 4356, 2021.
- [2] K. Aher, et al., "Preliminary study in irrigational quality of groundwater sources in parts of Soygaon block, District Aurangabad, India," Int. Res. J. Earth Sci., vol. 3, no. 2, pp. 7–12, 2015.
- [3] A. A. Faisal and Z. T. Abd Ali, "Groundwater protection from lead contamination using granular dead anaerobic sludge bio sorbent as permeable reactive barrier," Desalination Water Treat., vol. 57, no. 9, pp. 3891–3903, 2016.
- [4] D. Sethi and A. Di Molfetta, Groundwater Engineering: A Technical Approach to Hydrogeology, Contaminant Transport and Groundwater Remediation. Cham, Switzerland: Springer, 2019.
- [5] S. Maskey, et al., "Groundwater remediation strategy using global optimization algorithms," J. Water Resour. Plan. Manage., vol. 128, no. 6, pp. 431–440, 2002.
- [6] D. A. Da'ana, et al., "Removal of toxic elements and microbial contaminants from groundwater using low-cost treatment options," Curr. Pollut. Rep., vol. 7, no. 3, pp. 300–324, 2021.
- [7] Z. K. Abd Al-Hussain and H. M. Abdul-Hameed, "Removal of lead ions from wastewater by using a local adsorbent from charring tea wastes," Iraqi J. Chem. Petroleum Eng., vol. 24, no. 3, pp. 93–102, 2023.
- [8]H. M. Abdul-Hameed, "Adsorption of Cd(II) and Pb(II) ions from aqueous solution by activated carbon," Al-Khwarizmi Eng. J., vol. 5, no. 4, pp. 13–17, 2009.
- [9] D. Gusain and F. Bux, Batch Adsorption Process of Metals and Anions for Remediation of Contaminated Water. Boca Raton, FL, USA: CRC Press, 2021.
- [10] P. Chamoli, et al., "Characteristics of graphene/reduced graphene oxide," in Handbook of Nanocomposite Supercapacitor Materials I: Characteristics, pp. 155–177, 2020.
- [11] V. Karthik, et al., "Graphene-based materials for environmental applications: A review," Environ. Chem. Lett., vol. 19, no. 5, pp. 3631–3644, 2021.
- [12] H. Amjada, et al., "Design and modelling of water filtration assembly incorporating graphene embedded membrane," 2022.
- [13] L. Zhao, et al., "Advances in the applications of graphene adsorbents: From water treatment to soil remediation," Rev. Inorg. Chem., vol. 39, no. 1, pp. 47–76, 2019.
- [14] C. Xu, et al., "Graphene-based electrodes for electrochemical energy storage," Energy

- Environ. Sci., vol. 6, no. 5, pp. 1388–1414, 2013.
- [15] C.-P. Liang, et al., "Application of factor analysis for characterizing the relationships between groundwater quality and land use in Taiwan's Pingtung Plain," Sustainability, vol. 12, no. 24, p. 10608, 2020.
- [16] S. Wang, et al., "Adsorptive remediation of environmental pollutants using novel graphene-based nanomaterials," Chem. Eng. J., vol. 226, pp. 336–347, 2013.
- [17] K. Rawat and S. K. Singh, "Water quality indices and GIS-based evaluation of a decadal groundwater quality," Geol. Ecol. Landscapes, vol. 2, no. 4, pp. 240–255, 2018.
- [18] S. Shukla and A. Saxena, "Groundwater quality and associated human health risk assessment in parts of Raebareli district, Uttar Pradesh, India," Groundwater Sustain. Dev., vol. 10, p. 100366, 2020.
- [19] M. Zaman, et al., "Irrigation water quality," in Guideline for Salinity Assessment, Mitigation and Adaptation Using Nuclear and Related Techniques, pp. 113–131, 2018.
- [20] O. N. Mohammed and H. M. Abdulhameed, "Groundwater remediation for irrigation at Al-Raaed station using banana peel-derived activated carbon," Int. J. Des. Nat. Ecodyn., vol. 19, no. 6, pp. 1887–1899, 2024.
- [21] B. H. Graimed and Z. T. Abd Ali, "Batch and continuous study of one-step sustainable green graphene sand hybrid synthesized from date-syrup for remediation of contaminated groundwater," Alexandria Eng. J., vol. 61, no. 11, pp. 8777–8796, 2022.
- [22] S. K. Mustafa, et al., "Soft robotic actuation facilitated by polypyrrole coated-sulfonated polyvinyl alcohol-graphene oxide-ZnO network-based nanocomposite membranes," J. Polym. Environ., vol. 32, no. 3, pp. 1354–1366, 2024.
- [23] H. Algul, et al., "The effect of graphene content and sliding speed on the wear mechanism of nickel–graphene nanocomposites," Appl. Surf. Sci., vol. 359, pp. 340–348, 2015.
- [24] L. Stobinski, et al., "Graphene oxide and reduced graphene oxide studied by the XRD, TEM and electron spectroscopy methods," J. Electron Spectrosc. Relat. Phenom., vol. 195, pp. 145–154, 2014.
- [25] Z. T. Abd Ali, "Using activated carbon developed from Iraqi date palm seeds as permeable reactive barrier for remediation of groundwater contaminated with copper," Al-

- Khwarizmi Eng. J., vol. 12, no. 2, pp. 34–44, 2016.
- [26] H. M. Abdul-Hameed and I. N. Abeed, "Removal of copper from simulated wastewater by applying electromagnetic adsorption for locally prepared activated carbon of banana peels," J. Eng., vol. 23, no. 1, pp. 1–7, 2017.
- [27] R. K. Liew, et al., "Production of activated carbon as catalyst support by microwave pyrolysis of palm kernel shell: a comparative study of chemical versus physical activation," Res. Chem. Intermed., vol. 44, pp. 3849–3865, 2018
- [28] X. Liu and H. Luo, "Preparation of coal-based graphene by flash Joule heating," ACS Omega, vol. 9, no. 2, pp. 2657–2663, 2024.
- [29] L. Eddy, Flash Graphene Synthesis: Optimization, Scaling, and Thermodynamics. Houston, TX, USA: Rice Univ., 2023.
- [30] Z. Sun and Y. Hu, "Ultrafast, low-cost, and mass production of high-quality graphene," Angew. Chem. Int. Ed., vol. 59, 2020.
- [31] J. Ramírez, et al., "Design and construction of a high-current capacitor bank for flash graphene synthesis," Eng. Proc., vol. 47, no. 1, p. 18, 2023.
- [32] K. M. Wyss, et al., "Large-scale syntheses of 2D materials: flash joule heating and other methods," Adv. Mater., vol. 34, no. 8, p. 2106970, 2022.
- [33] P. A. Advincula, et al., "Flash graphene from rubber waste," Carbon, vol. 178, pp. 649–656, 2021.
- [34] K. M. Wyss, Flash Joule Heating for Nanomaterials Synthesis, Waste Upcycling, and Hydrogen Production. Houston, TX, USA: Rice Univ., 2023.
- [35] C. Girish and V. R. Murty, "Residence time distribution studies and modelling of phenol adsorption onto Lantana camara in packed bed," Int. J. Civil Eng. Technol., vol. 8, no. 10, pp. 1728–1738, 2017.
- [36] N. Ayawei, et al., "Modelling and interpretation of adsorption isotherms," J. Chem., vol. 2017, p. 3039817, 2017.
- [37] M. A. Al-Ghouti and D. A. Da'ana, "Guidelines for the use and interpretation of adsorption isotherm models: A review," J. Hazard. Mater., vol. 393, p. 122383, 2020.
- [38] P. Ganesan, et al., "Application of isotherm, kinetic and thermodynamic models for the adsorption of nitrate ions on graphene from aqueous solution," J. Taiwan Inst. Chem. Eng., vol. 44, no. 5, pp. 808–814, 2013.

- [39] S. Ahmed, et al., "Characterization and application of synthesized calcium alginate-graphene oxide for the removal of Cr<sup>3+</sup>, Cu<sup>2+</sup> and Cd<sup>2+</sup> ions from tannery effluents," Cleaner Water, p. 100016, 2024.
- [40] S. Wang, et al., "Adsorptive remediation of environmental pollutants using novel graphene-based nanomaterials," Chem. Eng. J., vol. 226, pp. 336–347, 2013.
- [41] V. B. Mbayachi, et al., "Graphene synthesis, characterization and its applications: A review," Results Chem., vol. 3, p. 100163, 2021.
- [42] M. G. Stanford, et al., "Flash graphene morphologies," ACS Nano, vol. 14, no. 10, pp. 13691–13699, 2020.
- [43] A. I. Bakti, et al., "Characterization of active carbon from coconut shell using X-ray diffraction (X-RD) and SEM-EDX techniques," J. Penelit. Fisika Aplikasinya (JPFA), vol. 8, no. 2, pp. 115–122, 2018.
- [44] C. Manoratne, et al., "XRD-HTA, UV visible, FTIR and SEM interpretation of reduced graphene oxide synthesized from high purity vein graphite," Mater. Sci. Res. India, vol. 14, no. 1, pp. 19–30, 2017.
- [45] D. Ratih and R. Siburian, "The performance of graphite/N-graphene and graphene/N-graphene as electrode in primary cell batteries," 2018.
- [46] A. Y. Alyami and A. Mahmood, "Synthesis, characterization and application of chitosan functionalized and functional graphene oxide membranes for desalination of water by pervaporation," Environ. Res., vol. 251, p. 118589, 2024.
- [47] M. Strankowski, et al., "Polyurethane nanocomposites containing reduced graphene oxide, FTIR, Raman, and XRD studies," J. Spectrosc., vol. 2016, p. 7520741, 2016.
- [48] Z. A. Naser and H. M. Abdul-Hameed, "Removal of Cu(II) from industrial

- wastewaters through locally-produced adsorbent prepared from orange peel," Caspian J. Environ. Sci., vol. 20, no. 1, pp. 45–53, 2022.
- [49] P. Kaewmee, et al., "Effective removal of cesium by pristine graphene oxide: Performance, characterizations and mechanisms," RSC Adv., vol. 7, no. 61, pp. 38747–38756, 2017.
- [50] V. Quintano, et al., "Long-range selective transport of anions and cations in graphene oxide membranes, causing selective crystallization on the macroscale," Nanoscale Adv., vol. 3, no. 2, pp. 353–358, 2021.
- [51] S. Ray, et al., "Bentonites as a copper adsorbent: Equilibrium, pH, agitation, dose, and kinetic effect studies," J. Hazard. Toxic Radioact. Waste, vol. 24, no. 1, p. 04019027, 2020.
- [52] F. Mazloomi and M. Jalali, "Ammonium removal from aqueous solutions by natural Iranian zeolite in the presence of organic acids, cations and anions," J. Environ. Chem. Eng., vol. 4, no. 1, pp. 240–249, 2016.
- [53] Y. Liu, et al., "Removal of Cr(VI) from wastewater using graphene oxide chitosan microspheres modified with α–FeO(OH)," Materials, vol. 15, no. 14, p. 4909, 2022.
- [54] Rathi, B. S. and P. S. Kumar . "Application of adsorption process for effective removal of emerging contaminants from water and wastewater," Environmental Pollution 280: 116995, 2021.
- [55] N. H. Barbhuiya, et al., "The future of flash graphene for the sustainable management of solid waste," ACS Nano, vol. 15, no. 10, pp. 15461–15470, 2021.
- [56] C. Jia, et al., "Graphene environmental footprint greatly reduced when derived from biomass waste via flash Joule heating," One Earth, vol. 5, no. 12, pp. 1394–1403, 2022.

#### تصنيع وتصنيف الجرافين الوميضي المستخدم لتقليل الملوثات في المياه الجوفية

#### نورة صبحي رحيم "، حيدر محمد عبد الحميد "

المناسبة البيئية، كلية الهندسة، جامعة بغداد، بغداد nawra.sobhi2311@coeng.uobaghdad.edu.iq \*البريد الالكتروني:

#### المستخلص

ان هذا البحث من المؤمل ان يحقق هدف تقييم سلوك فعالية الجرافين الوميضي المستخدم في عملية تحسين وتقليل قيمة (الاس الهيدروجيني والتوصيل الكهربائي وتراكيز الكتيونات والحديد) في المياه الجوفية الحقيقية التي تم اخذها من ابار محطة بحوث الرائد وهذه المياه تستخدم في قطاع الزراعة و استصلاح الاراضي ، وعلى ان تصل التراكيز للملوثات بعد تقليليها في المياه الجوفية الحقيقة الى مستوى تركيز مساوي للمعايير العراقية ومنظمة الاغنية والزراعة العالمية لمياه الري .تم استخدام الجرافين الوميضي في تجارب الدفعات بتقتية الامتزاز وهو مادة ذات اساس كاربوني عالية المسامية لها قابلية امتزاز عالية بسبب المساحة السطحية الفعالة البالغة (١٠/٥) م٢/غم. تم تصميم وتصنيع جهاز لتحضير الجرافين الوميضي والذي يحوّل الكاربون المنشط المحضر من الشكل السطحي للجرافين الوميضي ومجاميع الامتزاز الفعالة له تم توصيفها ب تحليل(REX, XRD, EDX) ، ان فعالية الامتزاز في تجارب النفعات كانت ٦٩٪ للكالسيوم و ٦٩٪ للمغنسيوم و ٢١٪ للمواد الصلبة الذائبة و ٠٠٠٪ للحديد عند اعلى كمية للمادة المستخدمة البالغة (١٠٥) مم من المياه الجوفية ولمدة ٤ ساعات وبسرعة اهتزازية (١٠٥) دورة في الدقيقة عند قيمة (٧) للاس الهيدروجيني . ان قابلية الامتزاز للجرافين الوميضي والتي تطابقت مع موديل (Freundlich) كانت الكالسيوم = ١٠٤٠ منعام عوديل محددة تم تغييرها وتعديلها الامتزاز الموريضي المصنع كان ضمن عوامل محددة تم تغييرها وتعديلها باستمرار (كمية المادة المازة ، سرعة الاهتزاز، زمن التلامس بين المادة المازة والعناصر الملوثة في المياه و الاس الهيدروجيني للمياه الجوفية لتراكيز الكتيونات والحديد والمواد الصلبة الذائبة الكلية وقيمة التوصيل الكهربائي والاس الهيدروجيني وفقا للمعايير المحددة في نهاية هذه التجارب